Heliyon 10 (2024) e27147

Contents lists available at ScienceDirect

Heliyon

journal homepage: www.cell.com/heliyon

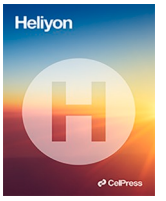

Research article

FOXM1 promotes the progression of non-small cell lung cancer by inhibiting miR-509-5p expression via binding to the miR-509-5p promoter region

Mengcha Tian [a], Jiaming Li [a], Huihui Wu [a], Yuying Wu [b,*]

[a] Department of Clinical Laboratory, Quanzhou First Hospital Affiliated to Fujian Medical University, Quanzhou, 362000, China
[b] Department of General Medicine, Quanzhou First Hospital Affiliated to Fujian Medical University, Quanzhou, 362000, China

ARTICLE INFO

Keywords:
Non-small cell carcinoma
FOXM1
miR-509-5p
Promoter
Inhibitors

ABSTRACT

Background: Forkhead box M1 (FOXM1) functions as a transcription factor and is consistently overexpressed in various cancers, including non-small-cell lung-, breast-, cervical-, and colorectal cancer. Its overexpression is associated with poor prognosis in patients with non-small-cell lung cancer, although the detailed mechanisms by which FOXM1 promotes the development of non-small-cell lung cancer remain unclear.
Objective: The mechanism of FOXM1 in migration, invasion, apoptosis, and viability of lung cancer cells was investigated.
Methods: Transwell assay, scratch test, and flow cytometry were employed to study the effects of FOXM1 on migration, invasion, and apoptosis in A549 cells. A quantitative polymerase chain reaction was used to determine the impact of FOXM1 on miR-509-5p expression in A549 cells. Dual-luciferase reporter gene assay and chromatin immunoprecipitation were adopted to investigate the molecular mechanisms of FOXM1 on miR-509-5p expression.
Results: FDI-6 (a FOXM1 inhibitor) reduced the protein abundance of FOXM1, thereby increasing the expression of miR-509-5p in A549 cells. Moreover, FDI-6 treatment significantly reduced migration, invasion, and viability of A549 cells while promoting cell apoptosis. Furthermore, miR-509-5p inhibitor obviously alleviated the biological effects of FDI-6 on A549 cells, suggesting that FOXM1 primarily exerted its cancer promoting effect by regulating miR-509-5p. Mechanistically, FOXM1 directly bound to the miR-509-5p promoter to inhibit miR-509-5p expression.
Conclusion: FOXM1 directly binds to the promoter region of miR-509-5p to form a negative feedback loop, thereby inhibiting miR-509-5p expression and promoting the development of non-small-cell lung cancer. This study is expected to complement research on the pathogenesis of non-small-cell lung cancer and promote the development of novel therapeutic targets for this disease.

1. Introduction

Lung cancer is a leading cause of cancer-related deaths worldwide [1], accounting for approximately 18.4% of total cancer deaths, and non-small cell lung cancer (NSCLC) accounts for 85% of all lung cancers diagnosed [2]. Currently, patients with NSCLC often undergo surgery, chemotherapy, and radiotherapy, although prognosis remains unsatisfactory [3]. An effective treatment for NSCLC

* Corresponding author.
E-mail address: 57565399@qq.com (Y. Wu).

https://doi.org/10.1016/j.heliyon.2024.e27147
Received 18 October 2023; Received in revised form 7 February 2024; Accepted 25 February 2024
Available online 27 February 2024

remains elusive owing to the unclear pathogenesis of NSCLC [4,5]. Therefore, an in-depth exploration of NSCLC pathogenesis can promote the development of new therapeutic targets and tumor markers and improve the clinical efficacy of treatments [6]. Forkhead box M1 (FOXM1) is a transcription factor that is overexpressed in various cancers, including NSCLC-, breast-, cervical, and colorectal cancer [7,8]. FOXM1 overexpression is associated with poor prognosis in patients with lung cancer [9–11]. Downregulation of FOXM1 expression can reduce cancer cell migration and invasion [12]. However, the mechanism of FOXM1 in the development of NSCLC remains unclear.

Studies should focus on miRNA to elucidate the role and mechanism of FOXM1 in the pathogenesis of cancer as tumor suppressors (such as miRNA, RB, and P53) reduce FOXM1 expression. miRNA is a small noncoding RNA that regulates gene expression after transcription by inhibiting translation or inducing target mRNA degradation. Abnormal miRNA expression occurs in lung cancer, some of which act as tumor suppressor genes [13]. The miR-509 family plays a tumor suppressive role in various cancers [14]. For example. miR-509-5p inhibits cell proliferation in NSCLC [15–17]. Mechanistically, the *FOXM1* gene may be the target of the miR-509-5p tumor suppressor as miR-509-5p binds to the 3′ untranslated region of *FOXM1* mRNA [18]. However, it remains unclear whether FOXM1 negatively regulates miR-509-5p expression.

This study aimed to reveal the role of FOXM1 in the regulation of miR-509-5p expression and its impact and molecular mechanism in the occurrence and development of NSCLC. We found that FOXM1 directly binds to the promoter region of miR-509-5p, forming a negative feedback loop, thereby inhibiting the expression of miR-509-5p and promoting the development of NSCLC. This study is expected to supplement the research on the pathogenesis of NSCLC and promote the development of novel therapeutic targets for NSCLC.

2. Materials and methods

2.1. Drugs and reagents

F–12K (Product number: 21127-022) was purchased from Gibco, USA; fetal bovine serum (FBS; Product number: SH30084.03) was purchased from HyClone, USA; phosphate-buffered saline (PBS; Product number: C10010500BT) was purchased from Life Technologies, USA; and trypsin (Product number: 25200072) was purchased from Gibco; and double antibody (Cat. No.: SV30010) was purchased from HyClone. A Cell Counting Kit-8 (CCK-8) detection kit (Cat. No.: CK-4) was purchased from Dojindo Laboratories, Japan; FDI-6 (Cat. No.: HY-112721) was purchased from MedChemExpress, USA; and an miR-509-5p inhibitor designed by Beijing Qingke Biotechnology Co., Ltd.; TsingZol. Total RNA Extraction Reagent (Product No.: TSP401), SynScript™ III cDNA Synthesis Mix (Product No.: TSK3225), 2 × TSINGKE® Master qPCR Mix (SYBR Green I) (Product No.: TSK201), and dNTPs Mix (10 mM each) (Product No.: TSK2200) were purchased from Beijing Qingke Biotechnology Co., Ltd. The Annexin V-Alexa Fluor 647/PI Cell Apoptosis Detection Kit (Cat. No.: 40304ES60) was purchased from Shanghai Yisheng Biotechnology Co., Ltd.; jetPRIME Transfection Reagent (Product No.: PT-114-75) was purchased from Polyplus, Germany; paraformaldehyde fixative (Neutral) (Product No.: G1101) was purchased from Wuhan Servicebio Technology Co., Ltd.; BD Matrigel (Product No.: 356234) was purchased from Shanghai Keya Biotechnology; crystal violet (Product No.: C0121) was purchased from Shanghai Beyotime Biotechnology Co., Ltd.; Trypan blue (Product No.: 15250061); and T-PER™ Protein extraction kit (Product No.: 78510) and the ChIP kit (Product No.: 26157) were purchased from Thermo Fisher Scientific, USA; Vectors including pcDNA3.1(+), pGL3 basic, pGL3-miR-509-5p and pcDNA3.1 (+)-FOXM1 were synthesized by BGI Tech Solutions (Beijing) Co., Ltd. All other reagents were of domestic analytical grade.

2.2. Instruments

The following instruments were used: Multiskan MK3 microplate reader (Thermo Fisher); Neofuge 15R refrigerated centrifuge (Shanghai Heal Force Company); HF90 CO_2 constant temperature incubator (Shanghai Heal Force Company); CKX53 inverted microscope (Olympus, Japan); HF-1200LC biosafety cabinet (Shanghai Heal Force Company); 5702R low-speed centrifuge (Eppendorf, Germany); Cellometer mini cell counter (Nexcelom, Germany); CytoFLEX S analytical flow cytometer (Beckman Coulter, USA); JY600C electrophoresis instrument (Jinan Junyi Biotechnology Co., Ltd.); YC-80 rolling shaker (Hangzhou Miou Instrument Co., Ltd.); JY92-IIN cell ultrasonic breaker (Ningbo Xinzhi Biotechnology Co., Ltd.); HSC-2015L desktop high-speed refrigerated centrifuge (Ningbo Xinzhi Biotechnology Co., Ltd.); SM-*M*-MCT2 magnetic stand (Shanghai Lixi Technology Co., Ltd.); QuantStudio 12 K real-time fluorescence quantitative PCR instrument (Applied Biosystems, USA); K5600 ultra-micro spectrophotometer (Beijing Zhongkemeng Technology Co., Ltd.); A300 PCR instrument (Hangzhou LongGene Scientific Instrument Co., Ltd.); and JY300 Horizontal Electrophoresis instrument (Beijing Junyi Dongfang Electrophoresis Equipment Co., Ltd.).

2.3. Cell lines

The A549 cell line (Cat. No.: CL-0016) was purchased from Procell Life Science & Technology Co., Ltd. (China).

2.4. Cell treatment

Lung cancer A549 cells were cultured in F–12K medium supplemented with 10% FBS and 1% penicillin/streptomycin at 37 °C and 5% CO_2. After passaging the cells twice, the culture medium was removed. The cells were washed with PBS and digested with trypsin for 2 min. The cell suspension was homogenized by gentle pipetting, centrifuged at 1000 rpm for 5 min, and resuspended in the

medium. Subsequently, 20 μL of trypan blue was added to the cell suspension for counting. Approximately 3.5×10^5 cells/well were added to a six-well plate in triplicate and incubated overnight with 5% CO_2 at 37 °C [19].

2.5. Western blotting

Total A549 cell protein was extracted using the T-PER™ Protein extraction kit. The extracted protein was quantified and electrophoresed, transferred to a polyvinylidene difluoride (PVDF) membrane, and blocked with 5% milk/TBST for 1 h at room temperature with shaking. Primary antibody was added and the membrane was incubated overnight at 4 °C. Subsequently, the secondary antibody was added, and the samples were incubated for 2 h at room temperature. The enhanced luminol and oxidizing reagents were diluted with ddH_2O, mixed well, and dropped onto a parafilm. The PVDF membrane was exposed to the electrochemiluminescence liquid to develop the color, and the results were observed using a gel imaging system. The gray value of the protein band was analyzed, and the relative expression of the target protein was calculated using GAPDH as an internal reference [20].

2.6. Transfection

A549 cells were transfected with miR-509-5p. jetPRIME buffer (200 μL), mimic inhibitor (200 nM), and jetPRIME reagent (4 μL) were added into EP tubes and incubated for 10 min at room temperature. Subsequently, the solution was added to the cell culture medium (500 μL), followed by incubation at 37 °C for 24 h. The medium was then replaced with fresh culture medium and re-incubation followed at 37 °C and % CO_2 for 24 h transfection for subsequent detection of FOXM1 mRNA and miR-509-5p expression [21].

2.7. Scratch test

Following transfection, cell scratches were made perpendicular to the well plate using a 10-μL pipette tip. Subsequently, the cell culture medium was removed, and the plate was washed thrice with PBS to remove the cell debris. The cells were suspended in serum-free medium and incubated at 37 °C and 5% CO_2. The cells were photographed at 0, 24, and 48 h, and the results were analyzed as previously described [22]. Three experimental groups (blank [control], FDI-6 + negative control [NC] inhibitor, and FDI-6 + miR-509-5p inhibitor) were evaluated [23].

2.8. Transwell cell migration assay

The Matrigel was thawed overnight at 4 °C, diluted 5 × with serum-free medium, and 50 μL was added to each Transwell chamber. The plate was incubated for 30 min at 37 °C. The A549 cells were incubated for 48 h and digested for 1 min. The cells were centrifuged at 1000 rpm for 5 min, and the supernatant was discarded. The cells were washed twice with PBS, resuspended in serum-free medium, and the cell density was adjusted to 1.5×10^5/mL. The cell suspension (200 μL) was added into the upper Transwell chamber and 600 μL was added to the lower chamber. Medium containing 10% FBS (μL) was added, and the cells were cultured for 48 h at 37 °C. The culture medium was replaced with fresh medium, and the cells were washed twice with PBS. The cells were stained with crystal violet for 10 min and washed twice with PBS. The cells in the upper chamber were wiped with a cotton swab. The migrating cells were observed using a microscope. Three randomly selected fields of view were used; the cells were counted, and pictures were captured as previously described [24].

2.9. Flow cytometry

Cells were pelleted via centrifugation for 5 min at 200 *g* and 4 °C. Subsequently, the cells were washed with pre-cooled PBS and centrifuged for 5 min at 200 *g* and 4 °C (2 ×). The PBS was discarded, and the cells were resuspended in 1 × Binding Buffer (100 μL), followed by the addition of Annexin V-Alexa Fluor 647 (5 μL) and propidium iodide (PI; 10 μL) and gently mixed. The cells were incubated for 15 min at room temperature in the dark. Subsequently, 1 × Binding Buffer (300 μL) was added and mixed well. The samples were placed on ice and analyzed using flow cytometry within 1 h [25].

2.10. CCK-8 assay

The CCK-8 solution (10 μL) was added to each well followed by incubation for 3 h at 37 °C and 5% CO_2. The absorbance value of each well was measured at 450 nm using a microplate reader. The results were analyzed as previously described [26].

2.11. Quantitative real-time polymerase chain reaction (RT-qPCR)

Total RNA was extracted from cells and reverse-transcribed into cDNA. PCR was performed according to the instructions in the 2 × TSINGKE® Master qPCR Mix. The reaction system comprised 2 μL reverse transcription product, 10 μL SYBR Green Mix, 0.8 μL forward and reverse primers, and 6 μL sterile water. The cycle conditions were as follows: 95 °C for 10 s, 60 °C for 60 s, 72 °C for 10–15 s, and 40 cycles at 72 °C. Fluorescence signals were collected. GAPDH and U6 were used as internal references respectively. The $2^{-\Delta\Delta Ct}$ method was used to analyze changes in gene expression, as previously described [27].

2.12. Dual luciferase reporter assay

Three experimental groups were established: pcDNA3.1(+) + pGL3 basic; pcDNA3.1(+) + pGL3-miR-509-5p; and pcDNA3.1 (+)-FOXM1 + pGL3-miR-509-5p. 293T cells (7×10^4 cells/well) were inoculated into a 24-well culture plate (in triplicate in a 500 μL cell suspension) and incubated at 37 °C. The next day, each group was separately transfected, and luciferase activity was detected 48 h after transfection according to the manufacturer's instructions [28].

2.13. Chromatin immunoprecipitation (ChIP)-qPCR experiment

A549 cells were harvested, and 37% formaldehyde was added to the cells at a final concentration of 1%. The reaction was terminated with 1× glycine. We subsequently collected the cell pellets and performed ultrasonic disruption, with fragmented DNA lengths between 200 and 1000 bp for immunoprecipitation (IP). The digested chromatin-containing supernatant (5 μL) was transferred to a centrifuge tube. The remaining 95 μL of the supernatant was transferred into 410 μL of 1X IP Dilution Buffer. The cells were incubated with antibodies for 2 h to overnight (depending on the antibody) at 4 °C. The positive control IP included anti-RNA polymerase II antibody (10 μL), whereas normal rabbit IgG (1 μL) was included as NC. The typical concentration for each target-specific IP was 5 μg antibody. Following incubation, the cells were vortexed. The ChIP-grade protein A/G magnetic bead tube was used to obtain a homogeneous suspension, and magnetic beads (20 μL) were added for 2 h at 4 °C. Following incubation, the beads were collected using a magnetic stand. The supernatant was discarded, and the cells were washed with IP wash buffer. Finally, the protein was digested with proteinase K and the DNA immunoprecipitated with the target protein was harvested, purified, and detected using qPCR [29]. The primer sequences are listed in Table 1.

2.14. Statistical analysis

The experimental data were statistically analyzed using the GraphPad Prism 8 software, and statistical significance was indicated as *, $P < 0.05$; **, $P < 0.01$; and ***, $P < 0.001$. Each experiment was repeated three times independently.

3. Results

3.1. FOXM1 inhibition upregulated miR-509-5p expression and inhibited migration, invasion, and viability of A549 cells

The FOXM1 inhibitor (FDI-6) was used to explore the potential role of FOXM1 in regulating miR-509-5p expression. The cells were exposed to different FDI-6 concentrations and the optimal inhibitory concentration was determined using western blotting analysis (Fig. 1**a**; Supplementary Fig. 1**a** and **b**). FDI-6 (5, 10, and 50 μM) significantly decreased FOXM1 expression in A549 cells (Fig. 1**b**, $P < 0.001$). Among them, 50 μM FDI-6 exhibited the best inhibitory effect on FOXM1. Therefore, this concentration was used in subsequent experiments.

We performed RT-qPCR to assess miR-509-5p expression in A549 cells to further determine the effect of FOXM1 on miR-509-5p expression. miR-509-5p expression in A549 cells significantly increased after FDI-6 treatment (Fig. 2), suggesting that FOXM1 inhibition increased the expression of miR-509-5p.

Subsequently, we investigated the effects of FOXM1 on migration, invasion, and viability of NSCLC to further confirm that they are mainly attributed to regulating miR-509-5p expression. A miR-509-5p inhibitor was also employed to confirm the role and mechanism of FOXM1 in the pathogenesis of lung cancer. The results of the cell scratch experiment showed that the cell migration rate in the FDI-6 + NC inhibitor group was significantly reduced compared with the blank group ($P < 0.05$). However, the migration rate of A549 cells showed an increasing trend after co-treatment with FDI-6 and miR-509-5p inhibitor (Fig. 3**a** and **b**). The Transwell chamber assay indicated that the numbers of invasive cells in the blank, FDI-6 + NC inhibitor, and FDI-6 + miR-509-5p inhibitor groups were 195 ± 6.43, 76 ± 5.13, and 164 ± 15.63, respectively (Fig. 3**c** and **d**). The invasion ratios in the FDI-6 + NC inhibitor and FDI-6 + miR-509-5p inhibitor groups and the blank group were 39.08% ± 0.03 and 76.79% ± 0.08, respectively, and the differences were statistically significant ($P < 0.05$). The CCK-8 detection results suggested that co-treatment with FDI-6 and NC inhibitor reduced viability in A549

Table 1
Primer pair and sequence list.

Name	Sequence(5′–3′)	Size	Interval
P-miR-509-1	GAGGGGAAGGTGGTGTTTCT AAGATGTCAACTCTTCTCAGCA	137 bp	636–772
P-miR-509-2	TCTCAAACTTTCCCACTTCCA TGGCATTAAGGGGTTAGAAGGA	124 bp	945–1068
P-miR-509-3	GGCATCTCTAGACCACAAGC ACACACAAGATCCTGAAAGCA	165 bp	1461–1625
P-miR-509-4	GCATCTCTAGACCACAAGCTCA CTCTACTCTGGAACCACAAAGT	197 bp	1462–1658
P-miR-509-5	TGTTGGATCTGAGGACTGCA TTCATCCCTCGAGTGCTATCC	150 bp	1723–1872

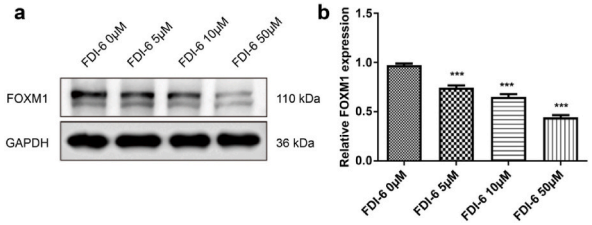

Fig. 1. Effect of different FDI-6 concentrations on FOXM1 expression in A549 cells.
a, Western blots; **b**, quantitative results of western blotting.The data in the bar diagrams are presented as the mean ± SD. Each experiment was repeated thrice independently; ***, $P < 0.001$ vs. the FDI-6 0 μM group).

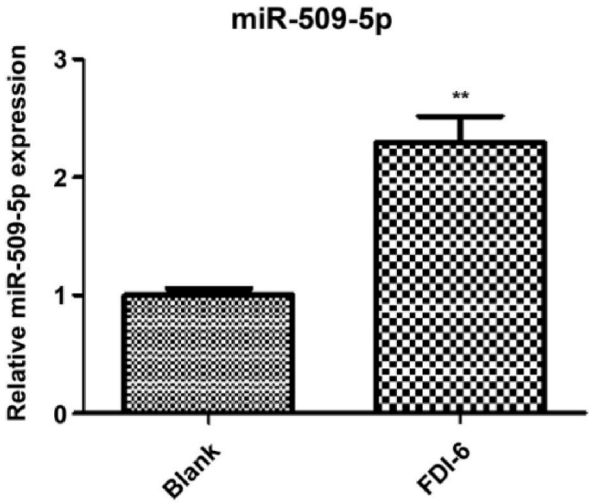

Fig. 2. Effect of FOXM1 on miR-509-5p expression in A549 cells. The data in the bar diagrams are presented as the mean ± SD. Each experiment was repeated thrice independently; **,
$P < 0.01$ vs. the Blank group).

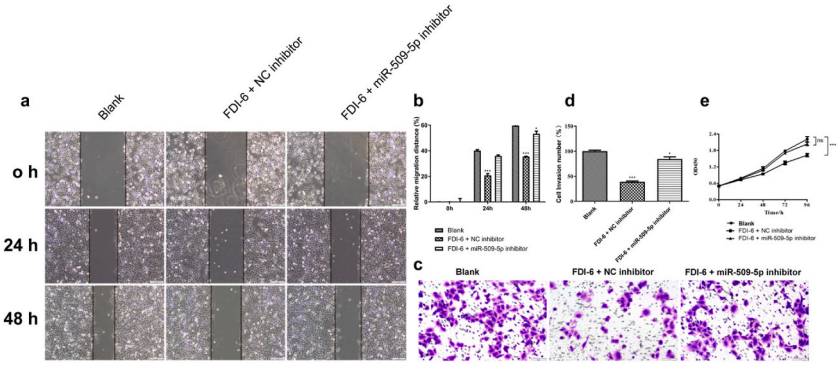

Fig. 3. Effect of FOXM1 on migration, invasion, and viability in A549 cells.
a and **b**, cell migration and quantitative results; **c** and **d**, cell invasion and quantitative results; **e**, cell viability. The data in the bar diagrams are presented as the mean ± SD. Each experiment was repeated thrice independently; *, $P < 0.05$; **, $P < 0.01$; and ***, $P < 0.001$ vs. the Blank group).

cells compared with the blank group, while cell viability in the FDI-6 + miR-509-5p inhibitor group was the same as that in the blank group (Fig. 3e). These results suggested that FOXM1 improved migration, invasion, and viability of A549 cells by decreasing miR-509-5p expression.

3.2. FOXM1 inhibition promoted cancer cell apoptosis by upregulating miR-509-5p expression

We subsequently examined whether the decreased miR-509-5p induced by FOXM1 promotes the apoptotic process given that FOXM1 improved the viability of cancer cells in vitro by regulating miR-509-5p expression. Flow cytometry results showed that the apoptosis rate in the blank group was 14.67% ± 1.09, while that in the FDI-6 + NC inhibitor and FDI-6 + miR-509-5p inhibitor groups was 36.28% ± 1.33 and 19.86% ± 1.57, respectively (Fig. 4**a** and **b**). These results indicated that the FDI-6 inhibitor significantly increased the apoptosis rate of A549 cells compared with the blank group ($P < 0.001$), while co-treatment with FDI-6 + miR-509-5p inhibitor resulted in apoptosis inhibition.

3.3. FOXM1 played a negative regulatory role by binding to the promoter region of miR-509-5p

We inserted the miR-509-5p promoter into the luciferase reporter vector (pGL3 basic), constructed an *FOXM1*-overexpression plasmid, and subcloned it into pcDNA3.1(+) to further explore how FOXM1 negatively regulates miR-509-5p expression. Subsequently, the *FOXM1* overexpression plasmid and reporter gene promoter plasmid were co-transfected into 293T cells for the dual-luciferase reporter gene experiments. Luciferase activity in the pcDNA3.1 (+) + miR-509-5p group was significantly upregulated ($P < 0.001$) compared to the pcDNA3.1 (+) + pGL3 basic group (Fig. 5**a**). Upregulation of luciferase activity was attenuated in the pcDNA3.1(+)-FOXM1+miR-509-5p group. These results indicated that FOXM1 may affect miR-509-5p promoter activity. FOXM1 was endogenously expressed in A549 cells using western blotting (Fig. 5**b;** Supplementary Fig. 2**a** and **b**) and bound to the promoter region of miR-509-5p according to ChIP-qPCR (Fig. 5**c**).

4. Discussion

FOXM1 is a member of the Forkhead box family of transcription factors that is overexpressed in a variety of cancers. This study confirmed that treatment with FDI-6 (FOXM1 inhibitor; 50 μM) significantly reduced FOXM1 expression in A549 cells (Fig. 1). Furthermore, FDI-6 reduced migration, invasion, and viability of A549 cells (Fig. 2), whilst increasing the apoptosis rate. These results are consistent with those of previous studies [18]. miRNAs play key roles in activating or inhibiting the occurrence and development of tumors. miR-509-5p inhibits tumorigenesis by inhibiting cancer cell proliferation and invasion in cervical, liver, and kidney cancers [15,16]. The miR-509-5p level is downregulated in NSCLCs, and miR-509-5p reduces the viability of NSCLC cells and inhibits their migration and invasion, suggesting that miR-509-5p plays a role in NSCLC development. It acts as a tumor suppressor by down-regulating the *FOXM1* gene [18]. miR-509-5p is a key tumor suppressor gene that is important for the study of NSCLC pathogenesis and the development of targeted drugs [17].

Fig. 2 showed that FOXM1 inhibits miR-509-5p expression. In support of this finding, co-treatment with FDI-6 and the miR-509-5p inhibitor resulted in increased migration, invasion, apoptosis, and viability rates of A549 cells (Fig. 2); thus, FOXM1 can inhibit miR-509-5p expression, thereby promoting the occurrence of NSCLC. Fig. 5 demonstrated that FOXM1 can bind to the miR-509-5p promoter region. In addition, we demonstrated that FOXM1 binds to the promoter region of miR-509-5p. In summary, this study highlights the possible mechanism by which miR-509-5p promotes the formation of A549 cells via FOXM1 (Fig. 5). FOXM1 promotes NSCLC by binding to the promoter region of miR-509-5p and inhibiting its transcription (Fig. 6). Additionally, Ma et al. [18] proposed that miR-509-5p may act as a tumor suppressor in the development of NSCLC by attenuating FOXM1 expression. Our results do not rule out the possibility that miR-509-5p inhibits the occurrence of NSCLC by reducing FOXM1 expression.

The limitations of this research were as described as follows: (1) This study used only epigenetic technologies (such as CHIP-qPCR), and the mechanisms might be not complete in this research. (2) This study used only one kind of NSCLC cell lines (A549). Based on the results of this study, we proposed three future research directions. First, this study verified the regulatory relationship between FOXM1

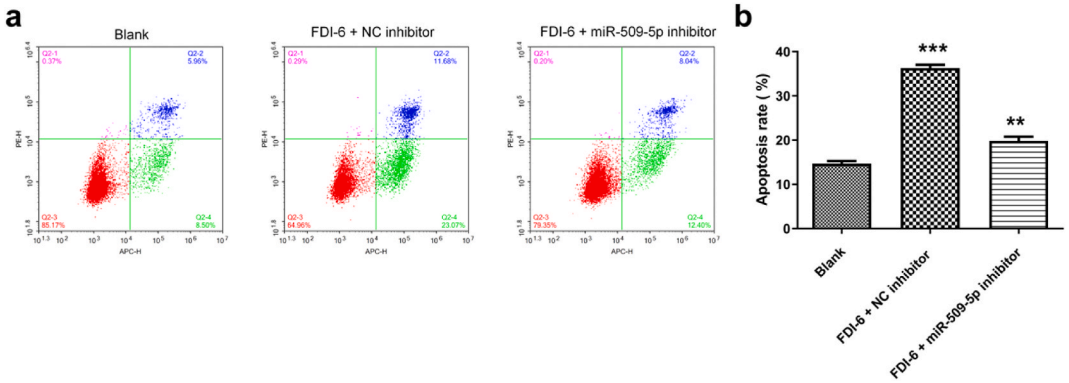

Fig. 4. Effect of FOXM1 on cell apoptosis in A549 cells.
a and **b**, cell proliferation and quantitative results. The data in the bar diagrams are presented as the mean ± SD. Each experiment was repeated thrice independently; **, $P < 0.01$; and ***, $P < 0.001$ vs. the Blank group).

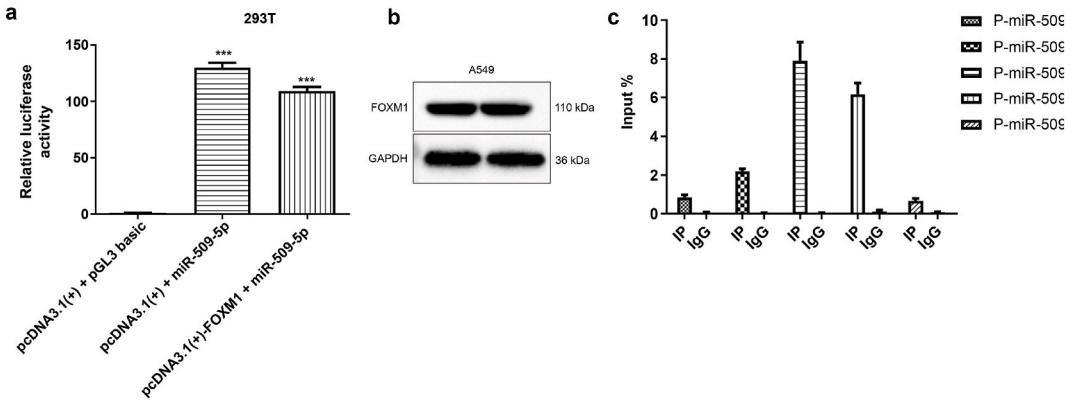

Fig. 5. FOXM1 bound the promoter region of miR-509-5p.
a, Quantification of luciferase activity; **b**, western blotting results of endogenous FOXM1 expression in A549 cells; **c**, ChIP-qPCR. The data in the bar diagrams are presented as the mean ± SD. Each experiment was independently repeated thrice; ***, $P < 0.001$ vs. the pcDNA3.1 (+) + pGL3 basic group). ChIP-qPCR: chromatin immunoprecipitation-quantitative PCR.

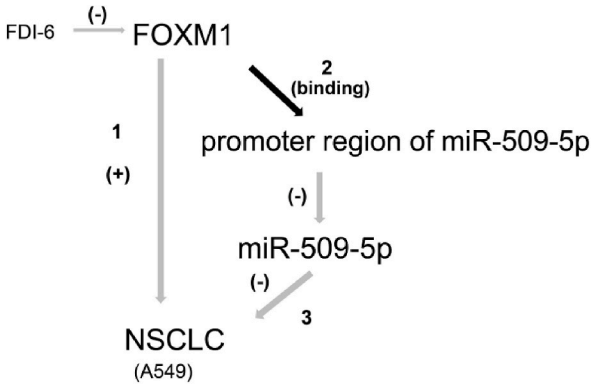

Fig. 6. The possible mechanism by which miR-509-5p promotes the occurrence of A549 through the *FOXM1* gene. FOXM1 was previously shown to promote the occurrence of NSCLC (pathway 1) [11]. This study found that FOXM1 can bind to the promoter region of the miR-509-5p gene to repress its transcription (pathway 2), thereby promoting the occurrence of NSCLC (pathway 3). The gray arrows indicate previous studies, and the black arrow denotes the main findings of this study.

and the miR-509-5p promoter by using epigenetic technologies such as CHIP-qPCR, thereby indirectly affecting miR-509-5p and A549 cells. Future research can try to directly study the regulatory effect of FOXM1 on miR-509-5p and other experiments about mutual regulation can be attempted as a confirmation method. In addition, although it has been reported that FDI-6 is an inhibitor that directly binds to the FOXM1 protein and can displace FOXM1 from the target genome and induce its subsequent transcriptional down-regulation, it cannot be ruled out that there may be some compound specificity issues. Therefore, gene knockout can be attempted as a confirmation method in the future. Finally, this study confirmed the changes in miR-509-5p after FOXM1 downregulation and its impact on A549 cells. Follow-up experiments can try to use other kinds of NSCLC cell lines to investigate biological roles and regulatory mechanism and upregulate FOXM1 through gene overexpression and other methods to verify the changes in miR-509-5p and its impact on A549 cells.However, these notion requires further investigation.

This study provides a new direction for researching the mechanism of FOXM1 promoting the occurrence of NSCLC and lays a theoretical foundation for developing novel therapeutic targets and improving NSCLC treatments.

Ethics statement

The A549 cell line (Cat. No.: CL-0016) was purchased from Procell Life Science & Technology Co., Ltd. (China).

Funding statement

This work was supported by the Quanzhou Science and Technology Plan Project (No. 2019N027S).

Data availability statement

Data will be made available on request.

CRediT authorship contribution statement

Mengcha Tian: Writing – original draft, Project administration, Methodology, Formal analysis, Data curation, Conceptualization. **Jiaming Li:** Methodology, Formal analysis, Data curation. **Huihui Wu:** Methodology, Formal analysis, Data curation. **Yuying Wu:** Writing – review & editing, Visualization, Project administration, Investigation, Funding acquisition.

Declaration of competing interest

The authors declare that they have no known competing financial interests or personal relationships that could have appeared to influence the work reported in this paper.

Appendix A. Supplementary data

Supplementary data to this article can be found online at https://doi.org/10.1016/j.heliyon.2024.e27147.

References

[1] X. Xie, C.C. Fu, L. Lv, et al., Deep convolutional neural network-based classification of cancer cells on cytological pleural effusion images, Mod. Pathol. 35 (2022) 609–614, https://doi.org/10.1038/s41379-021-00987-4.
[2] P. Wang, X. Fang, T. Yin, H. Tian, J. Yu, F. Teng, Efficacy and safety of Anti-PD-1 Plus Anlotinib in patients with advanced non-small-cell lung cancer after previous systemic treatment failure-a retrospective study, Front. Oncol. 11 (2021) 628124, https://doi.org/10.3389/fonc.2021.628124.
[3] Y. Ma, H. Liu, M. Zhang, et al., Successful treatment using targeted therapy, radiotherapy, and intrathecal chemotherapy in a patient with leptomeningeal metastasis with an epidermal growth factor receptor exon 20 insertion mutation: a case report, Ann. Palliat. Med. 11 (2022) 1533–1541, https://doi.org/10.21037/apm-21-321.
[4] S. Katakura, S. Murakami, Clinically-meaningful improvements in therapy for unresectable NSCLC, Expert Rev. Anticancer Ther. 22 (2022) 927–937, https://doi.org/10.1080/14737140.2022.2102483.
[5] A. Fariha, I. Hami, M.I.Q. Tonmoy, et al., Cell cycle associated miRNAs as target and therapeutics in lung cancer treatment, Heliyon 8 (2022) e11081, https://doi.org/10.1016/j.heliyon.2022.e11081.
[6] A. Chalmers, L. Cannon, W. Akerley, Adverse event management in patients with BRAF V600E-mutant non-small cell lung cancer treated with Dabrafenib plus Trametinib, Oncologist 24 (2019) 963–972, https://doi.org/10.1634/theoncologist.2018-0296.
[7] G.B. Liao, X.Z. Li, S. Zeng, et al., Regulation of the master regulator FOXM1 in cancer, Cell Commun. Signal. 16 (2018) 57, https://doi.org/10.1186/s12964-018-0266-6.
[8] N. Klinhom-On, W. Seubwai, K. Sawanyawisuth, et al., FOXM1c is the predominant FOXM1 isoform expressed in cholangiocarcinoma that associated with metastatic potential and poor prognosis of patients, Heliyon 7 (2021) e06846, https://doi.org/10.1016/j.heliyon.2021.e06846.
[9] I.M. Kim, T. Ackerson, S. Ramakrishna, et al., The Forkhead Box m1 transcription factor stimulates the proliferation of tumor cells during development of lung cancer, Cancer Res. 66 (2006) 2153–2161, https://doi.org/10.1158/0008-5472.CAN-05-3003.
[10] H. Madhi, J.S. Lee, Y.E. Choi, et al., FOXM1 Inhibition enhances the therapeutic outcome of lung cancer immunotherapy by modulating PD-L1 expression and cell proliferation, Adv. Sci. 9 (2022) e2202702, https://doi.org/10.1002/advs.202202702.
[11] Y. Wang, L. Wen, S.H. Zhao, Z.H. Ai, J.Z. Guo, W.C. Liu, FoxM1 expression is significantly associated with cisplatin-based chemotherapy resistance and poor prognosis in advanced non-small cell lung cancer patients, Lung Cancer 79 (2013) 173–179, https://doi.org/10.1016/j.lungcan.2012.10.019.
[12] A. Bowman, R. Nusse, Location, location, location: FoxM1 mediates β-catenin nuclear translocation and promotes glioma tumorigenesis, Cancer Cell 20 (2011) 415–416, https://doi.org/10.1016/j.ccr.2011.10.003.
[13] N. Kosaka, H. Iguchi, T. Ochiya, Circulating microRNA in body fluid: a new potential biomarker for cancer diagnosis and prognosis, Cancer Sci. 101 (2010) 2087–2092, https://doi.org/10.1111/j.1349-7006.2010.01650.x.
[14] S. Yoon, E. Han, Y.C. Choi, et al., Inhibition of cell proliferation and migration by miR-509-3p that targets CDK2, Rac1, and PIK3C2A, Mol. Cells 37 (2014) 314–321, https://doi.org/10.14348/molcells.2014.2360.
[15] W.B. Zhang, Z.Q. Pan, Q.S. Yang, X.M. Zheng, Tumor suppressive miR-509-5p contributes to cell migration, proliferation and antiapoptosis in renal cell carcinoma, Ir. J. Med. Sci. 182 (2013) 621–627, https://doi.org/10.1007/s11845-013-0941-y.
[16] Z.J. Ren, X.Y. Nong, Y.R. Lv, et al., Mir-509-5p joins the Mdm2/p53 feedback loop and regulates cancer cell growth, Cell Death Dis. 5 (2014) e1387, https://doi.org/10.1038/cddis.2014.327.
[17] P. Wang, Y. Deng, X. Fu, MiR-509-5p suppresses the proliferation, migration, and invasion of non-small cell lung cancer by targeting YWHAG, Biochem. Biophys. Res. Commun. 482 (2017) 935–941, https://doi.org/10.1016/j.bbrc.2016.11.136.
[18] N. Ma, W. Zhang, C. Qiao, et al., The tumor suppressive role of miRNA-509-5p by targeting FOXM1 in non-small cell lung cancer, Cell. Physiol. Biochem. 38 (2016) 1435–1446, https://doi.org/10.1159/000443086.
[19] M. Yu, B. Qi, W. Xiaoxiang, J. Xu, X. Liu, Baicalein increases cisplatin sensitivity of A549 lung adenocarcinoma cells via PI3K/Akt/NF-κB pathway, Biomed. Pharmacother. 90 (2017) 677–685, https://doi.org/10.1016/j.biopha.2017.04.001.
[20] S.Y. Jing, Z.D. Wu, T.H. Zhang, J. Zhang, Z.Y. Wei, In vitro antitumor effect of cucurbitacin E on human lung cancer cell line and its molecular mechanism, Chin. J. Nat. Med. 18 (2020) 483–490, https://doi.org/10.1016/S1875-5364(20)30058-3.
[21] M. Chakrabarti, S.K. Ray, Direct transfection of miR-137 mimics is more effective than DNA demethylation of miR-137 promoter to augment anti-tumor mechanisms of delphinidin in human glioblastoma U87MG and LN18 cells, Gene 573 (2015) 41–152, https://doi.org/10.1016/j.gene.2015.07.034.
[22] L. Liang, K. Hui, C. Hu, et al., Autophagy inhibition potentiates the anti-angiogenic property of multikinase inhibitor anlotinib through JAK2/STAT3/VEGFA signaling in non-small cell lung cancer cells, J. Exp. Clin. Cancer Res. 38 (2019) 71, https://doi.org/10.1186/s13046-019-1093-3.
[23] M.V. Gormally, T.S. Dexheimer, G. Marsico, et al., Suppression of the FOXM1 transcriptional programme via novel small molecule inhibition, Nat. Commun. 5 (2014) 5165, https://doi.org/10.1038/ncomms6165.
[24] L. Zhang, B. Liang, H. Xu, et al., Cinobufagin induces FOXO1-regulated apoptosis, proliferation, migration, and invasion by inhibiting G9a in non-small-cell lung cancer A549 cells, J. Ethnopharmacol. 291 (2022) 115095, https://doi.org/10.1016/j.jep.2022.115095.

[25] C. Sun, W. Gao, J. Liu, H. Cheng, J. Hao, FGL1 regulates acquired resistance to Gefitinib by inhibiting apoptosis in non-small cell lung cancer, Respir. Res. 21 (2020) 210, https://doi.org/10.1186/s12931-020-01477-y.
[26] L. Hou, S. Guan, Y. Jin, et al., Cell metabolomics to study the cytotoxicity of carbon black nanoparticles on A549 cells using UHPLC-Q/TOF-MS and multivariate data analysis, Sci. Total Environ. 698 (2020) 134122, https://doi.org/10.1016/j.scitotenv.2019.134122.
[27] Y.H. Lv, J.L. Ma, H. Pan, et al., RNA degradation as described by a mathematical model for postmortem interval determination, J. Forensic Leg. Med. 44 (2016) 43–52, https://doi.org/10.1016/j.jflm.2016.08.015.
[28] X. Wang, J. Wang, G. Huang, Y. Li, S. Guo, miR-320a-3P alleviates the epithelial-mesenchymal transition of A549 cells by activation of STAT3/SMAD3 signaling in a pulmonary fibrosis model, Mol. Med. Rep. 23 (2021) 357, https://doi.org/10.3892/mmr.2021.11996.
[29] F. Cao, M. Shi, B. Yu, X. Cheng, X. Li, X. Jia, Epigenetic mechanism of enrichment of A549 lung cancer stem cells with 5-Fu, OncoTargets Ther. 14 (2021) 3783–3794, https://doi.org/10.2147/OTT.S233129.